High-Frequency Monochromatic Acoustic Waves Generated by Laser-Induced Thermomodulation

E. P. N. Damen, A. F. M. Arts, and H. W. de Wijn
Faculty of Physics and Astronomy, and Debye Research Institute, Utrecht University, P.O. Box 80.000, 3508 TA Utrecht, The Netherlands
(Received 22 December 1995)

Monochromatic acoustic waves are produced in a single crystal of $PbMoO_4$ by periodic heating of a deposited Au film over an area about 40 μm in diameter by two interfering single-frequency dye lasers. Detection of these waves at optical difference frequencies up to 4 GHz is accomplished by Brillouin scattering. The generated power depends on the film thickness by acoustic interference within the film. Besides weak phonon defocusing effects, the divergence of the generated acoustic wave is limited by Fraunhofer diffraction.

PACS numbers: 63.20.−e, 78.35.+c

Progress in the physics of high-frequency phonons has been governed by the availability of suitable phonon generators and detectors. The simplest phonon generator is the plain heater [1], providing a Planckian spectrum, and so is the bolometer as detector. Various more sophisticated techniques have been developed, including microwave ultrasonics [2], electrostrictive mixing of laser beams [3], superconducting tunnel junctions [4], and transient heating [5]. These have yielded a wealth of information on subjects such as heat transport [6], Kapitza resistance [7], and phonon imaging [8]. Nevertheless, a technique capable of generating a monochromatic and directional high-frequency acoustic wave that is tunable in frequency is very much in need, if only because it would make genuine phonon spectroscopy feasible.

In this Letter, we present a new method for generating a monochromatic, tunable, and directional beam of high-frequency phonons. The method is based on thermomodulation, i.e., periodic thermal expansion of, in the present case, a metallic transducer. To achieve thermomodulation at high frequencies, the transducer is illuminated by two interfering single-frequency lasers operating at about equal intensities, but slightly different frequencies. The light incident on the transducer is accordingly modulated in intensity at the optical difference frequency. It produces a periodic variation in the temperature of the transducer, which in turn is converted into a strain wave via thermal expansion. It will first be demonstrated that thermomodulation indeed produces monochromatic phonons at the optical difference frequency. Subsequently, it is shown that the transducer acts as an acoustic interferometer, and that the acoustic beam injected into the crystal can serve to study "physical acoustics" quite analogously to physical optics. In particular, the beam is seen to diverge with distance according to Fraunhofer diffraction in conjunction with phonon focusing effects.

In the experiments, the beams of two cw frequency-stabilized single-frequency ring dye lasers are aligned to coincidence, and focused on the free surface of a thin (~400 nm) Au transducer deposited onto the single-crystalline specimen. For better adhesion, first a 4 nm thick intermediate layer of Cr was applied. The lasers operate with rhodamine 6G dye at a wavelength near 580 nm, and each of them produces light limited to a bandwidth of ~1 MHz with an output power of about 250 mW. The illuminated area of the metal film has a diameter of about 40 μm, and the modulation depth typically is 80%. All experiments were performed at room temperature, and so the generated monochromatic phonons coexist with a background of thermal phonons.

To investigate the intensity, the frequency, and the directionality of the generated phonons, reliance was made on Brillouin light scattering, using a setup of conventional design. The primary Brillouin beam was provided by a single-mode argon-ion laser delivering a power of ~200 mW. Optimal scattering efficiency was ensured by choosing as specimen a single crystal of lead molybdate ($PbMoO_4$; tetragonal unit cell; dimensions $10\times11\times9$ mm^3), which features a high acousto-optic constant. The acoustic wave reflects a minute fraction of the incoming laser beam, and, for anti-Stokes Brillouin scattering, the light frequency therefore is Doppler shifted upward by the phonon frequency. The scattering geometry, which is essentially determined by wave-vector conservation, is adjusted through the orientations of the primary Brillouin laser beam and the optical axis of the interferometer. It was set for the observation of longitudinal phonons of the desired frequency propagating along [001]. The scattered light was analyzed by the use of a quintuple-pass Fabry-Pérot interferometer, followed by a monochromator filtering out the laser plasma lines, and detected with a photomultiplier and standard photon counting techniques. The transmission curve of the interferometer was actively locked onto the position of the anti-Stokes line.

To demonstrate that thermomodulation generates a monochromatic acoustic wave, the anti-Stokes Brillouin scattering intensity was measured for a fixed Brillouin scattering geometry versus the frequency difference of the

0031-9007/95/74(21)/4249(4)$06.00

two ring dye lasers (Fig. 1). Note here that it is more practical to scan the optical difference frequency than the Brillouin geometry. The intensity is seen to reach its maximum at an optical difference frequency of 2.5 GHz, which indeed is the frequency for which the wave vector of the longitudinal phonons best fulfills the Brillouin condition pertaining to Fig. 1. The monochromaticity of the generated phonons is expected to be determined by the frequency spread of the dye lasers ($\sim$1 MHz [9]). Indeed, the width of the "line" in Fig. 1 (90 MHz) is essentially the instrumental resolution inclusive of the frequency selectivity of the interferometer and the finite opening angles of the optics. Brillouin scattering also detects thermal phonons of the appropriate wave vector, so that the generated phonons are seen on top of thermal ones. The ratio of the peak intensity over the thermal background was found to depend on the frequency, the temperature, the distance from the transducer, and the transducer thickness. At 300 K, ratios as high as 200 were observed.

A theoretical analysis may be based on concepts of classical physics [10]. Oscillatory heating causes a periodic expansion of the transducer, which in turn brings about an acoustic wave. In the present case of laser-induced heating, the energy is absorbed close to the surface, and next diffuses into the transducer. The skin depth associated with the oscillatory part of the heating

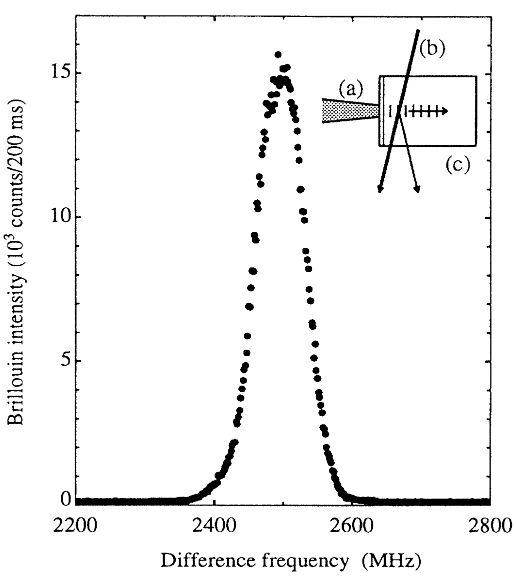

FIG. 1. The anti-Stokes Brillouin intensity versus the optical difference frequency. The 660 nm thick Au transducer is deposited on a (001) surface of a $PbMoO_4$ crystal. The intensity is maximum when the wave vector of the generated longitudinal phonons fulfills the Bragg condition. The thermal background is about 200 counts per dwell period of 200 ms. The inset schematically shows the geometry of the interfering laser beams (a), the Brillouin-scattering detection (b), and the crystal (c).

amounts to $\delta = (2K/\omega C_V)^{1/2}$, where K is the thermal conductivity, C_V is the specific heat, and ω is the angular optical difference frequency. For $\omega/2\pi = 4$ GHz, δ is of order 100 nm, which is less than the thickness d of the transducer ($d \geq 220$ nm). To simplify matters, we therefore adopt the approximation $\delta \ll d$. The oscillatory part of the temperature distribution may then be written

$$\vartheta(z,t) = \frac{\varphi_0}{(\omega K C_V)^{1/2}} \exp(-z/\delta + i\omega t), \tag{1}$$

where φ_0 is the amplitude of the total incident laser energy flux and the coordinate z measures the depth from the surface.

We next calculate the atomic displacement associated with $\vartheta(z,t)$ from the acoustic wave equation with the gradient of the thermal expansion as source. For the transducer this equation reads

$$\frac{\partial^2 u_1}{\partial z^2} - \frac{1}{v_1^2}\frac{\partial^2 u_1}{\partial t^2} = \beta \frac{\partial \vartheta(z,t)}{\partial z}, \tag{2}$$

where u_1 is the atomic displacement in the z direction, β is the thermal expansion coefficient, and v_1 is the longitudinal sound velocity. A similar equation without source term holds for the atomic displacement u_2 in the crystal. These two equations are solved for u_2 under the boundary conditions of a stress-free outer surface and balancing displacements u_i and stresses $C_i du_i/dz$ across the transducer-crystal interface. Here, C_i denotes the appropriate elastic constant C_{33} of the transducer ($i = 1$) or the crystal ($i = 2$). To derive the acoustic power flux Φ_{ac} injected into the crystal, we convert u_2 to the associated strain du_2/dz, and note that quite generally $\Phi_{ac} = \frac{1}{2}\rho v^3 \varepsilon^2$, in which ε is the amplitude of the strain, ρ is the mass density, and v is the longitudinal sound velocity. Using $\omega = q_1 v_1 = q_2 v_2$, with q_1 and q_2 the moduli of the phonon wave vectors, we finally find

$$\Phi_{ac} = \frac{\beta^2 K \rho_2 \omega \varphi_0^2}{2 C_V^3 v_1} \times \frac{(C_1/v_1)^2}{(C_1/v_1)^2 \sin^2 q_1 d + (C_2/v_2)^2 \cos^2 q_1 d}. \tag{3}$$

As already pointed out, the acoustic waves are produced near the free surface of the transducer, and subsequently travel toward the crystal. Because of acoustic mismatch they are reflected in part by the interface with the crystal, and next by the free surface [11]. By interference, therefore, a standing wave builds up, which shows itself in the denominator of Eq. (3). The generated acoustic power scales with φ_0^2. The efficiency of the generation furthermore scales with ω as long as $\delta \ll d$ and $\delta \ll 2\pi/q_1$, i.e., the phonon wavelength. Inserting [12] $\beta = 14 \times 10^{-6}$ K^{-1}, $K = 318$ W/mK, $C_V = 2.5 \times 10^6$ J/m^{3}K, $C_1 = 203$ GPa, and $v_1 = 3.24$ km/s for the Au transducer, and $\rho_2 = 6.95 \times 10^3$ kg/m^3, $C_2 = 91.7$ GPa, and $v_2 = 3.63$ km/s for the $PbMoO_4$ crystal, we find at acoustic resonance ($q_1 d = \pi$) the result $\Phi_{ac} = 8$ W/m^2

for 4 GHz and $\varphi_0 = 10^8$ W/m^2. Measurements of the Brillouin intensity have confirmed this estimate of Φ_{ac} as well as the quadratic dependence of Φ_{ac} on φ_0.

In the present case we have $C_1/v_1 \gg C_2/v_2$, i.e., the transducer-crystal interface acts as a fixed end, and so Φ_{ac} is maximum when a multiple of half the acoustic wavelength equals d. These resonances have been observed at various phonon frequencies by measuring the Brillouin intensity for a selection of d values. To accomplish this, a stepped gold transducer was deposited onto the crystal, providing thicknesses of 220, 330, 440, and 660 nm, and the crystal was displaced perpendicularly to the scattering plane over distances equal to the step width. This procedure conserves the Brillouin scattering geometry, and thus allows us to compare the intensities from one d to the next at a given phonon frequency. In Fig. 2, the experimental results are shown for phonon frequencies ranging from 2.5 to 4.0 GHz. The acoustic power is indeed found to peak at a smaller d for a larger phonon frequency, and in fact the resonances occur at the expected d. The wavelength of longitudinal 3.7 GHz phonons in Au, for instance, amounts to $2\pi v_1/\omega = 880$ nm, and so the first resonance occurs for $d = 440$ nm. In view of the inevitable paucity of d values, the resonances are best borne out by the agreement of Eq. (3) with the *complete* set of data. To show this, the theoretical Φ_{ac} as calculated from Eq. (3) vs d are inserted in Fig. 2, where for each plot only the vertical axis has been adjusted. Note that the approximation $\delta \ll d$ underlying Eq. (3) becomes invalid below $d \approx 100$ nm.

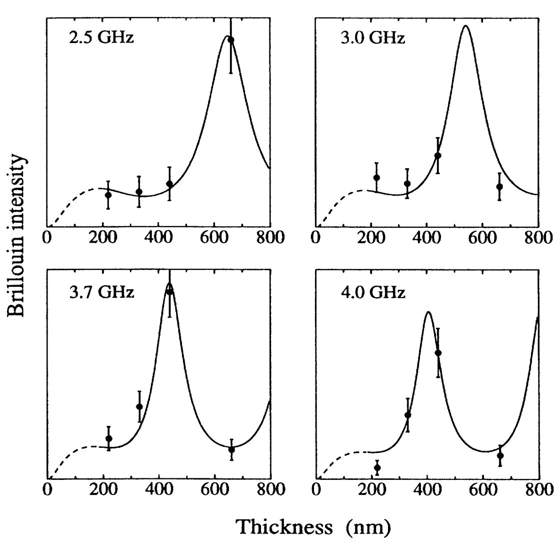

FIG. 2. The Brillouin intensity arising from the generated longitudinal phonons vs the thickness of the Au film at phonon frequencies of 2.5, 3.0, 3.7, and 4.0 GHz. The solid lines represent the intensity calculated from Eq. (3). Full-scale intensities are 15, 20, 30, and 40 $\times$ 10^3 counts/200 ms, respectively.

We have finally measured the divergence of the acoustic beam, to find that, apart from phonon focusing effects, it is essentially limited by Fraunhofer diffraction. Here, the Brillouin detection volume was narrowed down to the shape of a pencil, less than 10 μm in diameter and approximately 400 μm in length. This detection volume was scanned transversely through the beam and the Brillouin intensity was recorded for frequencies ranging from 1.2 to 4.0 GHz vs the displacement y at several distances z from the transducer. The results for 2.5 GHz are presented in Fig. 3. Note that the width increases only minutely over distances as large as $\sim$1 mm. In the actual experiments, the position of the illuminated disk at the transducer was moved by shifting the illuminating laser beams. It is furthermore noted that the wave-vector conservation inherent to Brillouin scattering is not limiting the intensities observed for the larger y in Fig. 3, as it is sufficiently relaxed by the narrowness of the Brillouin detection volume in proportion to the phonon wavelength λ_0. For 2.5 GHz, $\lambda_0 = 1.45$ μm in $PbMoO_4$.

The measured profiles in Fig. 3 are, within the experimental errors, of Gaussian shape. They represent the intensity profile of the acoustic beam convoluted with the intensity profile of the primary Brillouin laser beam. Note that both of these profiles are Gaussian, the acoustic one because the profiles of the dye-laser beams are so. The full $1/e$ width $2w(z)$ of the strain wave may thus be found from the relation $w_m^2(z) = \frac{1}{2}w^2(z) + w_B^2$, in which $2w_m$ is

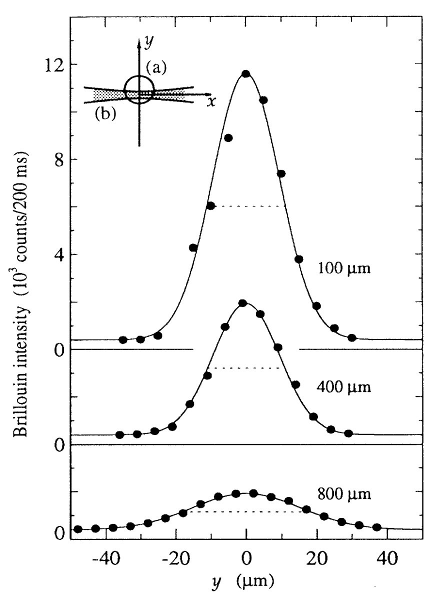

FIG. 3. The Brillouin intensity arising from the acoustic beam generated at 2.5 GHz vs the lateral position y at distances of 100, 400, and 800 μm from the transducer. The intensity is integrated over the x coordinate. The inset schematically shows the acoustic beam propagating along the z axis (a) and the primary Brillouin beam with the detection volume indicated (b).

TABLE I. Asymptotic angle of divergence α vs the phonon frequency ν. In calculating α_{th}, w_0 has been set to 18 μm.

ν (GHz)	α_{exp} (mrad)	α_{th} (mrad)
1.2	84 ± 3	82
1.7	59 ± 3	58
2.5	40 ± 3	39
4.0	24 ± 3	25

the measured $1/e$ width, $2w_B = 10 \pm 2$ μm is the $1/e$ width of the focused Brillouin laser beam, and the factor $\frac{1}{2}$ accounts for the fact that the acoustic power is proportional to the strain squared. For each frequency thus a series of $w(z)$ at various depths z is obtained. The gradual increase of their width with z may be characterized by the angular divergence at large depths $\alpha = dw(z)/dz|_{\infty}$. The results are collected in Table I. Note that α_{exp} is inversely proportional to ν.

Also inserted in Table I is the asymptotic angular divergence that follows from the acoustic analog of Fraunhofer diffraction in physical optics [13]. For a diffusive screen at $z = 0$ illuminated with a cylindrical Gaussian intensity profile of full $1/e$ width $2w_0$, we have

$$\alpha_{th} = \lambda_0/\pi w_0(1 - 2p). \qquad (4)$$

Here, phonon focusing effects, which result from anisotropy in the phonondispersion [14], are, for small angles, accommodated in the parameter p effectively modifying the length scale. The parameter p can be expressed in the elastic constants [15]. For longitudinal phonons propagating near the c axis in $PbMoO_4$, we find $p = 0.17$, i.e., the phonons are subjected to weak defocusing. Good agreement between α_{th} and α_{exp} is achieved for $w_0 = 18$ μm, which is only marginally larger than the value $w_0 = 16$ μm associated with the diffraction-limited focus of the dye-laser beams.

In summary; we have generated monochromatic high-frequency acoustic beams by periodic laser heating of a metallic transducer. These beams are tunable in frequency simply by varying the frequency of one of the dye lasers and are Fraunhofer diffracted with divergences of order 0.01 rad.

The work was supported by the Netherlands Foundation "Fundamenteel Onderzoek der Materie (FOM)" and the "Nederlandse Organisatie voor Wetenschappelijk Onderzoek (NWO)."

[1] R. J. von Gutfeld and A. H. Nethercot, Phys. Rev. Lett. **12**, 641 (1964).
[2] H. E. Bömmel and K. Dransfeld, Phys. Rev. Lett. **1**, 234 (1958); **3**, 83 (1959); Phys. Rev. **117**, 1245 (1960); E. H. Jacobsen, Phys. Rev. Lett. **2**, 249 (1959); J. Acoust. Soc. Am. **32**, 949 (1960).
[3] K. A. Nelson and M. D. Fayer, J. Chem. Phys. **72**, 5202 (1980); K. A. Nelson, D. R. Lutz, M. D. Fayer, and L. Madison, Phys. Rev. B **24**, 3261 (1981).
[4] W. Eisenmenger and A. H. Dayem, Phys. Rev. Lett. **18**, 125 (1967); H. Kinder, Phys. Rev. Lett. **28**, 1564 (1972); P. Berberich, R. Buemann, and H. Kinder, Phys. Rev. Lett. **49**, 1500 (1982); W. Eisenmenger, in *Physical Acoustics* (Academic Press, New York, 1976), Vol. VII, p. 79.
[5] C. Thomsen, H. T. Grahn, H. J. Maris, and J. Tauc, Phys. Rev. B **34**, 4129 (1986).
[6] E. T. Swartz and R. O. Pohl, Rev. Mod. Phys. **61**, 605 (1989).
[7] R. J. Stoner and H. J. Maris, Phys. Rev. B **48**, 16 373 (1993).
[8] G. A. Northrop and J. P. Wolfe, in *Nonequilibrium Phonon Dynamics,* edited by W. E. Bron (Plenum Press, New York, 1985), p. 165.
[9] This spread corresponds to a coherence length of the acoustic wave of about 1 mm.
[10] R. M. White, J. Appl. Phys. **34**, 3559 (1963).
[11] In experiments in the time domain [5], picosecond strain pulses generated with a pulsed laser have been observed to complete several round trips through the transducer.
[12] Y. A. Touloukian *et al., Thermophysical Properties of Matter* (IFI/Plenum, New York, 1970), Vols. 1, 4, 10, and 12; W. Pies and A. Weiss, in *Crystal Structure Data of Inorganic Compounds,* edited by K.-H. Hellwege and A. M. Hellwege, Landolt-Bornstein, New Series, Group III, Vol. 7, Pts. b1 and f (Springer-Verlag, Berlin, 1977); R. F. S. Hearman, in *Elastic Piezoelectric and Related Constants of Crystals,* edited by K.-H. Hellwege and A. M. Hellwege, Landolt-Bornstein, New Series, Group III, Vol. 11 (Springer-Verlag, Berlin, 1979).
[13] M. V. Klein and T. E. Furtak, *Optics* (Wiley and Sons, New York, 1985).
[14] B. Taylor, H. J. Maris, and C. Elbaum, Phys. Rev. B **3**, 1462 (1971); F. Rösch and O. Weis, Z. Phys. B **25**, 101 (1976); **25**, 115 (1976); A. G. Every, Phys. Rev. B **24**, 3456 (1981); **34**, 2852 (1986).
[15] H. J. Maris, in *Nonequilibrium Phonons in Nonmetallic Crystals,* edited by W. Eisenmenger and A. A. Kaplyanskii (North-Holland, Amsterdam, 1986), p. 51ff.